

Design of Improved Metal-Organic Framework (MOF) H₂ Adsorbents

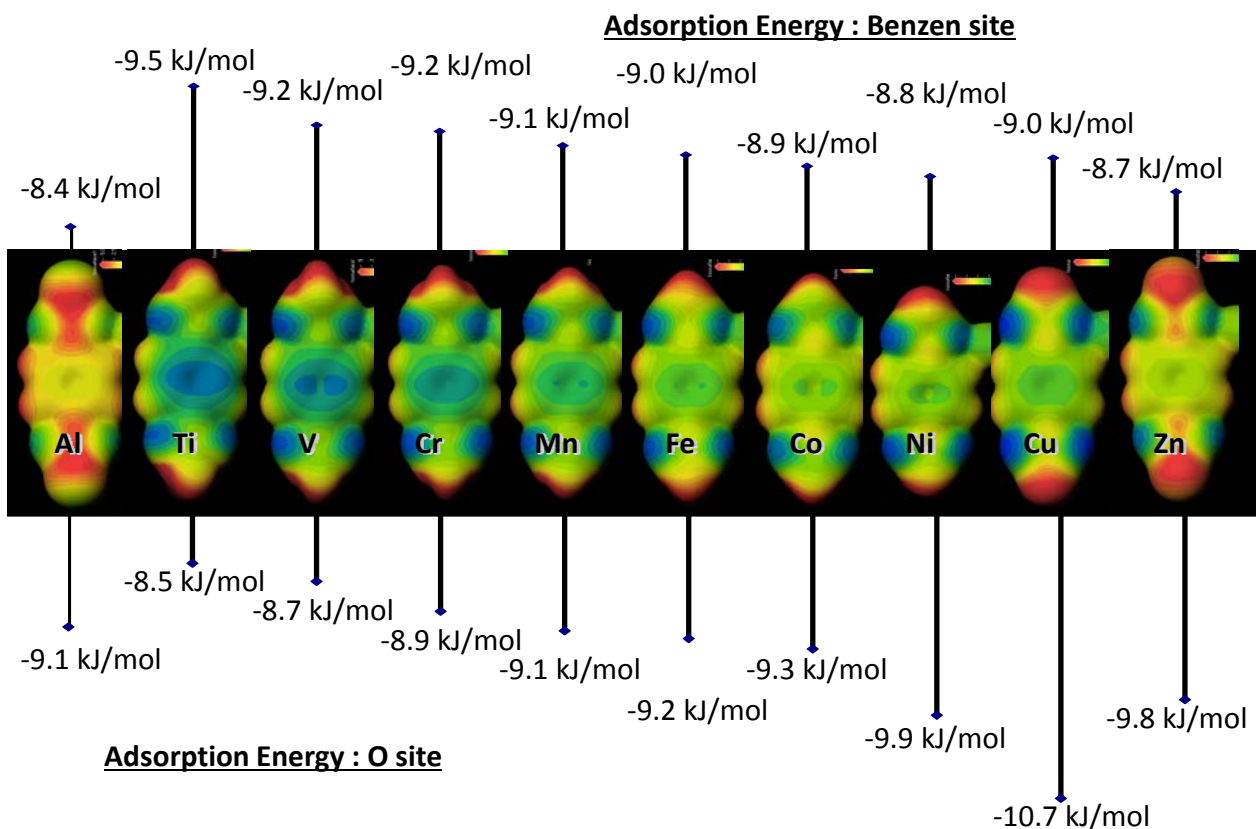
Terumi Furuta *, Izuru Kanoya, Hiroshi Sakai and Mitsuya Hosoe

S1. Details of MOF Structure Design

Hydrogen adsorbents for FCEV applications must have high gravimetric (wt %) and volumetric (vol %) storage densities, in addition to a low heat of adsorption (ΔH) to increase cruising distance, to decrease tank volume, and to reduce charging and discharging times. Typical strategies to increase hydrogen uptake are increasing the number of hydrogen adsorption sites and increasing the adsorption energy. The specific surface area in metal organic frameworks (MOFs) are often increased by selecting long organic linkers. However, this increase of specific surface area will lead to the addition of many pores, therefore the volumetric density tends to decrease, which leads to increased volume of the hydrogen storage tank on vehicles. Therefore, the increase in pore volume due to an increase of the length of organic linkers should be limited in order to not decrease the volumetric density. Our adsorption site analysis of IRMOF-1, based on neutron diffraction measurements and first principles density functional calculations, suggest that the major adsorption sites are around the metallic core [1], thus the metallic cores must be placed with a high density. More hydrogen can be adsorbed by increasing the hydrogen adsorption energy (heat of adsorption), but more heat will be generated during charging, thereby reducing the charging rate. The heat of hydrogen adsorption must be limited to approximately 10 kJ/mol H₂ for the charging time to be comparable to vehicles running on gasoline. The heat of hydrogen adsorption ΔH of IRMOF-1, a conventional MOF, is 4.8 kJ/mol H₂ (see Section S2), which is a low enough value. An increase in the amount of adsorbed hydrogen may be expected by designing a MOF with a higher heat of adsorption. Adsorption properties are known to increase by using hetero-organic ring linkers where some atoms are substituted by elements such as N, F or Cl. An analysis of the electron density around the adsorption sites obtained by first principles calculations also support this trend, suggesting that the hydrogen adsorption energy increases where electrons are localized (Figure S1). Therefore, including atoms with large electronegativity in linkers is a powerful strategy to increase hydrogen adsorption energy.

To increase the storage density, a reduction of the effective space occupied by the atoms and an increase in the adsorption energy are essential in the metallic cores. The paddle wheel structure is a good candidate to achieve this. It is a double-core structure with low coordination that reduces the space occupied by atoms in the core and that has sites with high adsorption energy from exposure of the metal. Adsorption energies of a double-core nucleus obtained by first principles calculation were 10 ~ 12 kJ/mol H₂ for most metals in the second to fourth period of the periodic table, and there was no significant difference in adsorption energy between different metals (Table S1). Therefore, we chose Cu as the metal because many organometallic complexes of Cu has been synthesized.

Figure S1. Electrostatic potential and adsorption energy.



* Calculated with VASP-LDA-PAW. ** The red areas correspond to positively charged areas and blue areas to negatively charged areas in the electrostatic potential map. The adsorption energy tends to be larger when there is more negative charge, or where the electrons are localized.

Table S1. Adsorption energy of paddle wheel.

Core Atom	Adsorption Energy / kJ/mol	Core Atom	Adsorption Energy / kJ/mol
Li	-11.3	Ni	-11.2
Be	-10.2	Cu	-11.3
B	-	Zn	-10.9
Na	-11.3	Ga	-
Mg	-10.7	Y	-10.2
Al	-12.2	Zr	-11.7
K	-	Nb	-11.7
Ca	-10.5	Mo	-10.9
Sc	-10.3	Rh	-11.4
Ti	-9.4	Pd	-11.3
V	-11.0	Cd	-
Cr	-11.0	La	-
Mn	-11.0	Ce	-
Fe	-11.3	Pt	-12.0
Co	-9.7		

* [-] Does not form paddle wheel structure. ** Value calculated with VASP-LDA-PAW.

The framework must have a high density of cores and also should form interconnected pores. Furthermore, the configuration need to be designed not to cover cap sites of the paddle wheel structure.

Therefore, we designed a layered framework where monolayers formed by a combination of triangles and hexagonal holes are stacked in an ABAB sequence. A high core density is made possible by the triangular frames, and displacing the A-layers and B-layers allow the triangular sites to form interconnected pores while not blocking the cap sites.

The bonding angle between paddle wheels and linkers is 90°, but as the bonding angles in the triangular framework are 60°, the framework is unstable but must nevertheless be stabilized. Therefore, the paddle wheels were tilted from a vertical orientation to minimize the deformation of the bonding angles, together with bent linkers.

The pore size must also be optimized to enhance the adsorption of hydrogen. Hydrogen uptake properties were increased by designing the size of pores in the MOF to be double the size of hydrogen molecules.

S2. Calculation Details for Adsorption Energies

All adsorption energies in this report were calculated using the following conditions:

Code: VASP (Vienna ab-initio simulation program)
 Potentials: LDA PAW
 * GGA method estimated a non-bonded energies (adsorption energies) very small.
 Therefore adsorption energies were estimated using LDA.
 k mesh: gamma point only
 Plane wave cutoff: 400 eV
 Scheme: $E_{\text{ads}} = E_{\text{frame}+\text{H}_2} - E_{\text{frame}} - E_{\text{H}_2}$;
 E_{ads} : adsorption energy;
 $E_{\text{frame}+\text{H}_2}$: Total energy of MOF with adsorption H₂;
 E_{frame} : Total energy of only MOF (without H₂);
 E_{H_2} : Total energy of only H₂ molecule.

S3. Measurement of Heat of Adsorption (ΔH) in IRMOF-1 and CuPDC

The heat of hydrogen adsorption ΔH was obtained from the van't Hoff equation given below

$$\ln \frac{P}{P_0} = \frac{\Delta H}{R} \cdot \frac{1}{T} - \frac{\Delta S}{R}$$

P [atm] Pressure of hydrogen in the system
 P_0 [atm] Pressure in the standard condition, usually 1 atm
 R Gas constant (8.31451 J/mol K)
 T [K] Thermodynamic temperature
 ΔH [J/mol] Change in enthalpy
 ΔS [J/mol K] Change in entropy

The heat of adsorption was calculated from Table S2: values given in the article and results from low temperature measurements are described in Section S4-b.

Table S2. The base data for ΔH .

	Uptake wt %	T K	P MPa	ΔH kJ/mol	ΔS J/mol K
IRMOF-1	0.60	77	0.0341	-4.8	-52.9
		82	0.0486		
		297.15	8.4560		
CuPDC	0.77	77	0.0081	-6.0	-57.5
		82	0.0168		
		297.15	8.9159		

S4-a. Consideration in the Case of Using H₂ Adsorption Property for FCEV

In this article, only physical properties of purely adsorbed hydrogen onto MOFs frameworks are discussed. In reality, hydrogen molecules, not adsorbed on frameworks but existing in the pores of MOF crystal have to be considered for FCEV application. In this case, the hydrogen uptake are IRMOF-1 8.6 g/L @ 8.9 MPa (crystal density = 0.61 g/cc) and CuPDC 9.7 g/L @ 8.9 MPa (crystal density = 1.196 g/cc) including gas hydrogen of MOFs pores. Therefore, CuPDC can load about 13% more hydrogen in FCEV than IRMOF-1.

S4-b. Low Temperature Hydrogen Storage Properties of CuPDC

The hydrogen uptake at low temperatures are given Figures S2 and S3.

Figure S2. Hydrogen uptake at 77 K. Solid line is for CuPDC, dashed line is for IRMOF-1. Measurements taken with an ASAP2020 apparatus.

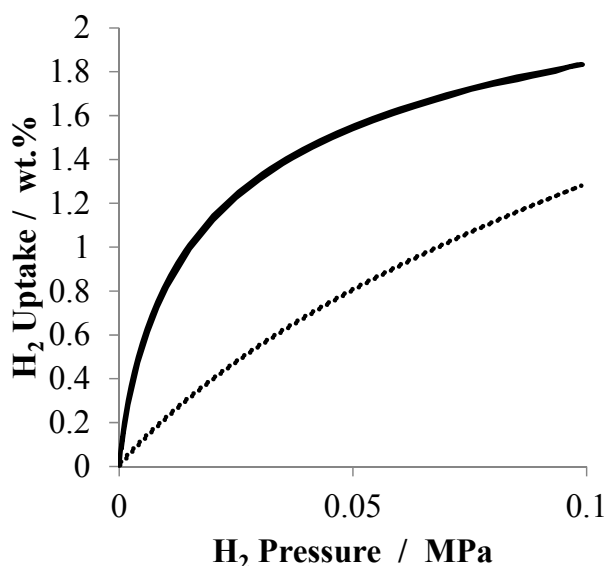
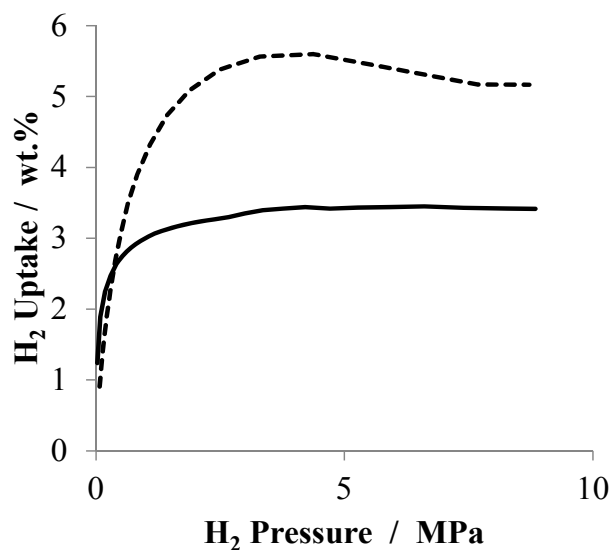


Figure S3. Hydrogen uptake at 80 K and under high pressure. Solid line is for CuPDC, dashed line is for IRMOF-1. PCT measurement equipment provided by Suzuki Shokan was used.



S5. Pore Ratio and Site Density of CuPDC

The pore ratio and site density was converted from the physical quantities in Table S3.

Pore ratio = [Cylinder Pore Volume (cc/g)] × [Crystal density (g/cc)]

Site density = [Site number /unit] / [Unit Volume (nm³/unit)]

Table S3. The base data for Pore Ratio and Site Density.

Formula units	Unit Volume (nm ³ /unit) [calc.]	Cylinder Pore Volume (cc/g) [exp.]	Crystal density (g/cc) [exp.]	Pore ratio [exp.]	Site number/unit [3] [calc.]	Site density (/nm ³) [calc.]
IRMOF-1 Zn ₄ O(BDC) ₃	2.114	1.412	0.61 [2]	0.86	6O site × 4, 3O site × 4 = 8	3.8
Cu ₂ PDC ₂ Cu ₂ PDC ₂	0.6768	0.413	1.196	0.49	Core site × 4, Cu-cap site × 1, N top site × 1 = 6	8.9

S6. Details of Structural Analysis of CuPDC with XRPD

Measured at Spring-8:

Beam line: 19B2
Wave length: 1.00083 Å
Energy: 16 keV

Details available at <http://www.spring8.or.jp/en/>.

S7. Details of Structural Analysis of CuPDC with Rietveld Refinement

(1) Conditions:

X-ray diffraction

Spectrix X'pert PRO MPD

Tube voltage: 45 kV Tube current: 40 mA CuK α

4 ~ 120 degree 0.0167 degree/step 240 s/step

Line width 15 mm (fixed)

Rapid X'Celerator detector + monochromator

Analysis

Space group P6₃mc (No.186)

Program RIETAN-2000

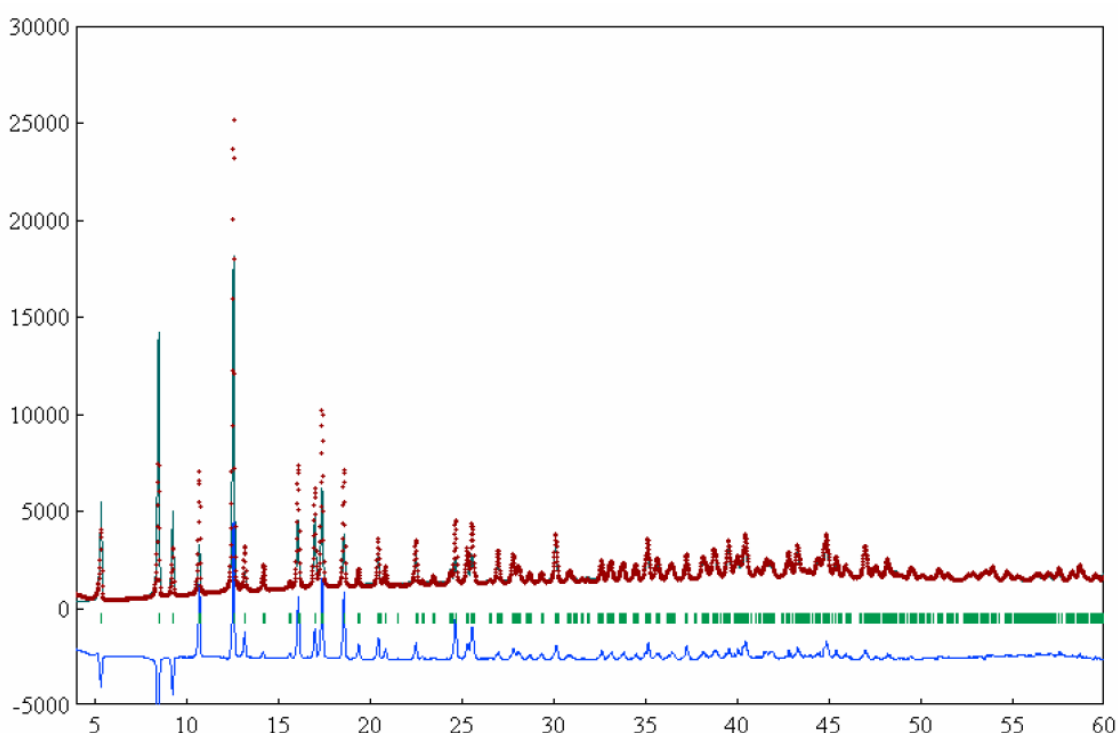
Structure factors of neutral atoms were used.

Spectrum between 4 ~ 60 degree used to roughly design model, spectrum up to 90 degree used for high precision determination of structure.

Initial model (Figure S4)

A simple model was built by starting from the structural model obtained from the single crystal analysis, then removing one pyridine of every two pyridines and removing hydrogen atoms.

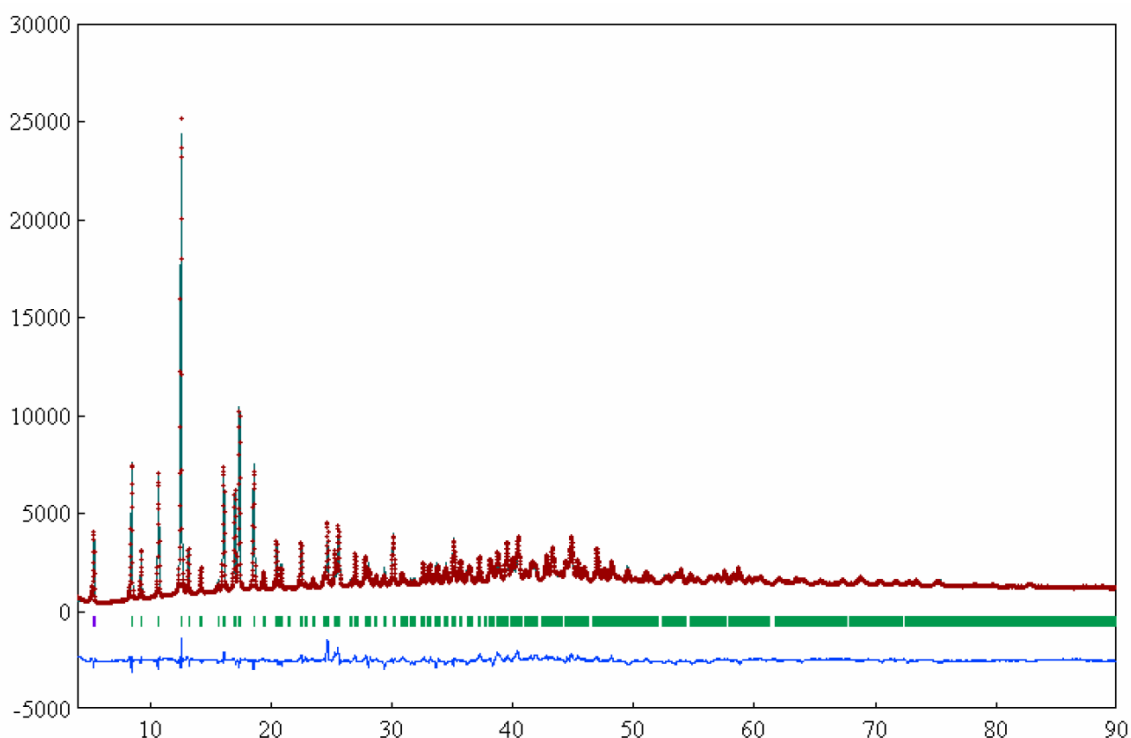
Figure S4. Comparison of simulations from single crystal analysis and XRD measurements.



(2) Results (Figure S5)

A model using an occupancy of 1 in Cu1 and PDC sites showed the most stable convergence and did not give irregular results, therefore this model was selected.

Figure S5. Rietveld refinement results.



The fitted lattice parameters given Table S4 show that the structure obtained by Rietveld analysis is compressed in the c-axis direction compared to that from single crystal analysis.

Table S4. Comparison of lattice parameters from single crystal analysis and Rietveld analysis.

Lattice parameter	a (Å)	c (Å)	V (Å ³)
Single crystal analysis	18.9975(10)	13.4566(9)	4,205.9(4)
Rietveld analysis	19.086(2)	13.4207(9)	4,234.1(6)

The small angle peak intensities can be reproduced better by increasing the site occupancy of oxygen (W5–W13 structure parameters) in pores to more than 1, therefore there may be guest molecules or residual precursors that did not react (molecules including heavy elements such as Cu).

In conclusion, the site occupancies in the crystal is estimated to be close to 1, implying there are very few defects in the crystal.

(3) Rietveld Refinement Results: Numerical Data (Table S5) and Number of each species in the unit cell and density (Table S6).

Table S5. Rietveld refinement results: Numerical data.

Reliability factors, goodness-of-fit indicator, and Durbin-Watson statistic							
Rwp	Rp	RR	Re	S	RI	RF	
5.10	3.74	16.40	2.49	2.0527	9.85	6.93	
Lattice parameters (Angstrom or degree) and unit-cell volume (Angstrom**3)							
a	b	c	alpha	beta	gamma	V	
19.08644	19.08644	13.42073	90.0000	90.0000	120.0000	4234.0562	
0.00170	-	0.00091	-	-	-	0.6063	
Structure parameters, g, x, y, z, B/Angstrom**2, and U/Angstrom**2							
	neq	*g	=n	x	y	z	B
Cu1	6	1.0000	6.0000	0.37907	0.18953	0.26419	2.655
	-	-	-	0.00040	-	0.00069	0.115
Cu2	6	1.0000	6.0000	0.29434	0.14717	0.09534	2.655
	-	-	-	0.00042	-	0.00068	-
C11	12	1.0000	12.0000	0.45920	0.03890	-0.01130	1.217
	-	-	-	-	-	-	0.236
C12	12	1.0000	12.0000	0.48200	0.08920	0.06940	1.217
	-	-	-	-	-	-	-
C13	6	1.0000	6.0000	0.55620	0.11240	0.11560	1.217
	-	-	-	-	-	-	-
C14	12	1.0000	12.0000	0.42850	0.11950	0.11180	1.217
	-	-	-	-	-	-	-
N11	6	1.0000	6.0000	0.50650	0.01300	-0.05140	1.217
	-	-	-	-	-	-	-
C14	12	1.0000	12.0000	0.42850	0.11950	0.11180	1.217
	-	-	-	-	-	-	-
N11	6	1.0000	6.0000	0.50650	0.01300	-0.05140	1.217
	-	-	-	-	-	-	-
O11	12	1.0000	12.0000	0.44430	0.15000	0.19760	1.217
	-	-	-	-	-	-	-
O12	12	1.0000	12.0000	0.37110	0.11220	0.05730	1.217
	-	-	-	-	-	-	-
C25	12	1.0000	12.0000	0.23810	0.17950	-0.10550	1.217
	-	-	-	-	-	-	-
C26	12	1.0000	12.0000	0.21990	0.17340	-0.20590	1.217
	-	-	-	-	-	-	-
C27	6	1.0000	6.0000	0.21160	0.10580	-0.25710	1.217
	-	-	-	-	-	-	-
C28	12	1.0000	12.0000	0.23620	0.02900	0.24490	1.217
N22	6	1.0000	6.0000	0.24690	0.12345	-0.05450	1.217
	-	-	-	-	-	-	-
O23	12	1.0000	12.0000	0.29620	0.07660	0.29770	1.217
	-	-	-	-	-	-	-
O24	12	1.0000	12.0000	0.22416	0.03980	0.15660	1.217
	-	-	-	-	-	-	-
W5	6	2.6085	15.6508	0.43892	0.21946	0.40400	47.673
	-	0.0663	0.3981	0.00190	-	0.00275	1.241
W6	2	2.9401	5.8802	0.00000	0.00000	0.31544	47.673
	-	0.1066	0.2133	-	-	0.00530	-
W7	2	0.4308	0.8616	0.00000	0.00000	-0.98063	47.673
	-	0.1115	0.2229	-	-	0.03618	-
W8	2	2.0096	4.0191	0.66667	0.33333	0.42015	47.673
	-	0.1070	0.2140	-	-	0.00583	-
W9	2	4.0826	8.1652	0.66667	0.33333	-0.20330	47.673
	-	0.0978	0.1955	-	-	0.00315	-
W10	6	0.5165	3.0987	0.88461	0.44231	0.19275	47.673
	-	0.0426	0.2555	0.00639	-	0.01174	-
W11	6	1.3429	8.0574	0.15834	0.07917	0.50100	47.673
	-	0.0395	0.2372	0.00326	-	0.00396	-
W13	6	2.8171	16.9027	0.78309	0.21691	-0.36719	47.673
	-	0.0489	0.2934	0.00053	-	0.00259	-

neq: number of equivalent points per unit cell. n: number of equivalent atoms per unit cell.

Table S6. Number and mass of each species in the unit cell, and density.

Atom	N *	At.wt. / 6.02214E23	=Mass
Cu	12.00000	63.54600	1.266247E-21 g
C	84.00000	12.01070	1.675316E-21 g
N	12.00000	14.00670	2.791040E-22 g
O	110.63582	15.99940	2.939331E-21 g
Total = 6.159998E-21 g			

$$d = \text{Total}/V = 6.159998\text{E}-21/4.234056\text{E}-21 = 1.454869 \text{ g/cm}^3.$$

References and Notes

1. Kanoya, I.; Furuta, T.; Sakamoto, R.; Hosoe, M.; Ichikawa, M.; Itoh, K.; Fukunaga, T. Anomalous Aggregation State of Deuterium Molecules in the Nanoscale Pores of a Metal Organic Framework. *J. App. Phys.* **2010**, *108*, 074310.
2. Eddaoudi, M.; Kim, J.; Rosi, N.; Vodak, D.; Wachter, J.; O’Keeffe, M.; Yaghi, O.M. Systematic Design of Pore Size and Functionality in Isorecticular MOFs and Their Application in Methane Storage. *Science* **2002**, *295*, 469-472.
3. The sites were counted to sites had over 10 kJ/mol adsorption energy by DFT calculation.